

Polarization-optical investigation of magnetization processes near dislocations in yttrium iron garnet single crystals

V. K. Vlasko-Vlasov, L. M. Dedukh, and V. I. Nikitenko

Institute of Solid State Physics, USSR Academy of Sciences

(Submitted February 21, 1973)

Zh. Eksp. Teor. Fiz. 65, 376-395 (July 1973)

Results are presented of an investigation of local changes in the magnetic characteristics of $Y_3Fe_5O_{12}$ ferrimagnetic single crystals near separate dislocations. The magnetization curves of crystal microregions adjacent to the atomic dislocation are measured. It is shown that the dislocation stress field induces an inhomogeneous distribution of the spontaneous magnetization vectors around it, affects their rotation induced by the external magnetic field and determines the configuration of the domains adjacent to the dislocation nucleus. Some features of the interaction kinetics of various types of domains with single edge dislocations are described. It is found that the nature of the interaction between the dislocations and domain walls not only depends on their mutual position but also on the type and orientation of the spontaneous magnetization vectors with respect to the dislocation Burgers vector. The results obtained are analyzed on the basis of existing theories. Some contradictions between the theoretical predictions and experimental facts are noted and discussed.

In spite of the remarkable progress towards explaining the phenomena that lead to magnetic ordering, there is still no consistent quantitative theory of the magnetization of ferromagnets. The foundations for the theory are contained in the well-known papers by Landau and Lifshitz^[1], who have shown that the thermodynamic-equilibrium state should correspond to a crystal broken up into domains such that the resultant magnetic moment of the sample is equal to zero in the absence of a field. Numerous experiments have shown convincingly that the sample becomes magnetized as a result of the displacement of the domain walls and rotation of the spontaneous-magnetization vectors. On the basis of these premises, the magnetism specialists started to develop a theory describing the behavior of ferromagnets in an external magnetic field.

The first estimates have shown immediately that the magnetization curve cannot be described by taking into account only the energies of the exchange and magnetic interaction. It turned out that an important role in the formation of the macroscopic characteristics of the magnetization curves of a real crystal is played by the magnetoelastic energy, which determines the change of the relativistic and exchange interactions under the influence of spatially inhomogeneous internal stresses that exist in the absence of external forces. The experimental data offered evidence that by thermomechanical working it is possible to change radically the form of the magnetization curves of crystals, to control their magnetic properties, and to produce magnetically hard materials with definite magnetic structures. However, the development of the theory of magnetization of ferromagnets was halted for several decades because the very concept of the internal stresses remained indeterminate for a long time.

The progress made in the physics of strength and plasticity by directly taking into account the real structure of crystals has made it possible to define more concretely the nature of the elementary sources of internal stresses. According to the dislocation concepts, the internal stresses are caused by imperfections of the crystal structure (dislocations, point defects, their clusters, etc.). The dislocations are the most important source of internal stresses, since each produces a slowly-decreas-

ing long-range field of internal stresses (the stresses due to a dislocation decrease in inverse proportion to the distance r from its center, whereas the stresses from an infinite chain of point defects decrease like $1/r^2$, while those from point defects and their clusters decrease like $1/r^3$). Depending on the mutual placement of the dislocations, the stresses caused by them can either add up to form macroscopic stresses that decrease over distances of the order of the dimensions of the crystal, or cancel each other and decrease over distances of the order of the distance between the dislocations (microstresses).

In accordance with these concepts, a concrete theory was developed^[2] for the effect of internal stresses on the magnetic properties of crystals^[3]. Naturally, it turned out that the final result depends radically not only on the type of the domain boundaries and the magnetic structure, but also on the character of the distribution and type of dislocations. Unsurmountable difficulties were therefore encountered when it came to an experimental verification of the fundamental premises of the theory for traditional magnetically-ordered crystals such as ferromagnetic metals. The main difficulty was that such samples could not be used to investigate simultaneously the dislocation structure and the magnetic structures, or to study their evolution and the kinetics of the interaction during the course of magnetization. The tremendous dislocation density in bulky metallic samples can be investigated directly only in an electron microscope. The domain structure is much larger in scale and can be investigated with an optical microscope. Furthermore, experiments yield information only on the magnetic structure of the surface layers.

It was first reported briefly in^[4,5] that the noted difficulties can be eliminated by research on transparent ferrimagnetic crystals, using the polarization-optical method for a simultaneous and direct study of the domain and dislocation structures of the samples.

We report here results of a quantitative investigation of the local changes of magnetic characteristics of ferrimagnetic yttrium iron garnet (YIG) single crystals near single dislocations. We describe a setup that makes it possible to reveal and analyze the microstress fields

around individual dislocations, to measure the magnetization curves of microscopic regions of the crystals, and to observe simultaneously the kinetics of the variation of the domain structure. Using this setup, we succeeded in measuring for the first time the magnetization curves of the local microscopic crystal regions adjacent to an atomic dislocation, and to study the features of the kinetics of the interaction of different types of domains with single edge dislocations. All the results are analyzed on the basis of the existing theories, and the contradictions between their predictions and the experimental facts are pointed out and discussed.

I. EXPERIMENTAL PROCEDURE

The investigated samples were single-crystal yttrium-iron garnet plates ($Y_3Fe_5O_{12}$) cut along the $\{110\}$ or $\{112\}$ plane and polished mechanically and chemically in orthophosphoric acid at $360^\circ C$. The plate thickness ranged from 0.1 to 0.4 mm.

To display the dislocations and to investigate the elastic fields produced by them we used a procedure described in [6]. When plane-polarized light is transmitted through the plate, the stress fields around the dislocations that are parallel to the direction of propagation of the light and having an edge component of the Burgers vector, give rise to characteristic birefringence rosettes, as a result of the piezo-optical effect [7]. From the forms of the rosettes we determined the direction of the dislocation line and its slip plane [8]. The sign of the Burgers vector was determined from an analysis of the black-white tone of the rosette, which is a result of the superposition of the Cotton-Mouton effect and the piezo-optical effect [9].

The domain structure in plane-polarized light was investigated on the basis of the magneto-optical effects [10]. From an analysis of the light passing through the domains we determined the longitudinal and transverse components of the magnetization vector M_s , which are responsible for the rotation of the plane of polarization of the light (the Faraday effect) and for the magnetic birefringence (the Cotton-Mouton effect), respectively. This has made it possible to decipher reliably the domain structure in the interior of the crystal.

The surface domain structure was investigated by the powder-figure method. A colloidal suspension was prepared by a method proposed by Elmore [11] and deposited on a chemically-polished surface of the sample. We examined powder figures in the light field in both reflected and transmitted light, simultaneously with the bulk domain structure revealed by the magneto-optical method.

The kinetics of the interaction of the domains with the dislocations was observed directly on the screen of an electron-optical converter (EOC) [4], or was photographed on motion-picture film and then carefully examined on a screen. The displacements of the domain boundaries were photographed frame by frame, the magnetic field being changed by an amount $\Delta H = 0.01$ Oe every 24 frames. The rate of change of the magnetic field was varied in a wide range. The same process was examined at different rates of change of the magnetic field (from 7 to 0.01 Oe/sec), both by motion-picture photography and directly on the screen of the microscope EOC. All the motors and magnet windings were fed from highly stabilized power supplies.

The schematic block diagram of the setup used to investigate the local magnetic characteristics and stress

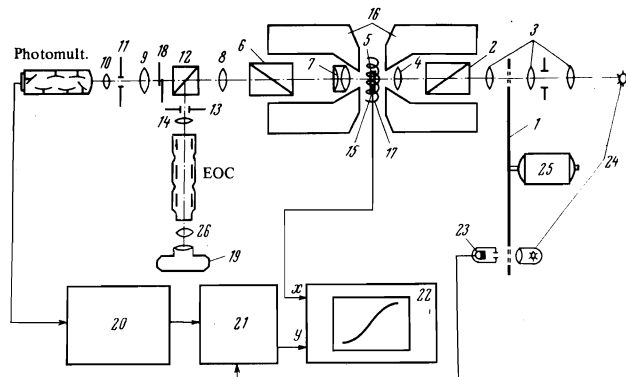


FIG. 1. Schematic block diagram of the setup for the study of the magnetization curves of local microsections of a ferrimagnet that is transparent in the visible and infrared, with simultaneous observation of the domain structure of the investigated sections: 1—disk with openings, 2, 6, Nicol prisms, 3, 8-10, 14—lenses, 4—condenser, 5—sample, 7—objective, 11, 13—diaphragms, 12—semitransparent mirror, 15—Hall pickup; 16—magnet, 17—solenoid, 18—shutter, 19—photographic camera, 20—narrow-band amplifier, 21—synchronous detector, 22—x-y recorder, 23—photodiode, 24—light source, 25—electric motor, 26—lens.

fields around the dislocations is shown in Fig. 1. The setup is based on the use of the piezo-optical and magneto-optical effects to reveal the dislocations and to study the magnetization curves, respectively. A light beam (from a high-intensity lamp with stabilized radiation) was modulated with a disk chopper 1, polarized by a Nicol prism 2, and focused with a system of lenses 3 and a condenser 4 on the investigated sample 5. The light passing through the sample was analyzed by Nicol prism 6 and directed through an optical system (objective 7 and lenses 8-10) through diaphragm 11 to the cathode of a photoelectric multiplier. A fraction of the beam was deflected by a semitransparent mirror 12 to a system used for direct observation of the photometry object. The object image obtained in infrared light was converted into visible light (with simultaneous amplification of the image brightness) by a high-sensitivity multistage EOC. A glass plate 13 on which a diaphragm is superimposed is placed between mirror 12 and the EOC; the image of the object on the photocathode of the EOC. That section of the field of view which was bounded by the image of the diaphragm 13 and was seen on the screen of the EOC corresponded to the section bounded by diaphragm 11 and directed to the cathode of the photomultiplier. The electric signal produced in the photomultiplier was amplified with a narrow-band amplifier and was fed through a synchronous detector to the vertical coordinate of an x-y automatic potentiometer recorder. The reference signal to the synchronous detector came from a photodiode illuminated by light modulated with the aid of disk 1. The horizontal coordinate of the potentiometer received a signal from the Hall pickup 15, which was mounted alongside the sample to record the magnetic field. The magnetization of the sample in the direction perpendicular to the light flux was produced by magnet 16, while solenoid 17 magnetized the crystal in a direction perpendicular to the light flux. The construction of the stage for the sample made it possible to move the latter (together with the Hall pickup and the solenoid) between the poles of the magnet 16 (the displacement was controlled with micrometric screws) and to rotate it about the optical axis. The Nicol prism 2 was provided with a dial and its rotation could be measured accurate to $15''$.

To reveal the dislocations in the crystal and to analyze the microstresses about them, the sample was magnetized with solenoid 17 in a plane perpendicular to the light flux. Under these conditions there was no Faraday effect, and the presence of the Cotton-Mouton effect produced a uniform illumination of the field of view, against the background of which we observed the characteristic birefringence rosettes caused by the dislocations (and by other stress sources)^[9]. After analyzing the microstresses and setting the required microscopic section of the crystal in the field of view of the diaphragm 13, the solenoid 17 was turned off, the shutter 18 was opened, and the setup was ready to record the magnetization curves.

When the sample was magnetized along the direction of propagation of the light, the value of the Faraday rotation α_F was proportional to the M_S component M_S^{\parallel} parallel to the light flux. The measurement was carried out in a position at which the angle θ between the planes of polarization of the Nicol prisms 2 and 6 was 45° . In this case one uses the most linear section of the squared sine wave describing the intensity of the transmitted light I as a function of the angle of rotation of the Nicol prisms θ ^[12], which certainly overlaps the interval of values of α_F when the investigated plates are fully magnetized ($\approx 7^\circ$).

Thus, the intensity increment of the light passing through the magnetized YIG plate depends linearly on M_S^{\parallel} and characterizes the state of the magnetization of the ferrimagnet. To eliminate the error due to the presence of the piezo-optical effect and magnetic birefringence, the magnetization curves were recorded with the magnetic field applied in the forward and backward directions^[12]. The analysis of the domain structure, the observation of its behavior, the photography, and the motion-picture photography of the displacement processes when the crystal was magnetized were all carried out directly on the EOC screen.

Thus, the described setup makes it possible to display and investigate the microstresses around individual dislocations, to study the behavior of domains in the elastic field near the dislocation, and to measure the magnetization curves in the surrounding regions of the crystal.

II. RESULTS AND DISCUSSION

1. Investigation of magnetization curves of local crystal microsections adjacent to an edge dislocation

A. Analysis of the change of the domain structure of a single-crystal YIG plate placed in a magnetic field. Figure 2a shows the domain structure, observed in plane-parallel light, of one of the YIG plates, 0.2 mm thick, cut along the $\{110\}$ plane. It consists of regions of spontaneous magnetization with vectors M_S along easy-magnetization directions of the type $\langle 111 \rangle$. At the chosen sample orientation (indicated in Fig. 2a), four directions of the type $\langle 111 \rangle$ lie in the plane of the plate, and four directions of the type $\langle 111 \rangle$ make an angle $\pm 55^\circ$ with this plane. The light domains are magnetized in the $\langle 111 \rangle$ directions that do not lie in the plane of the plate (we call them "Faraday" domains, since their light coloring is due to the large rotation of the polarization plane). These domains occupy the bulk of the crystal and are designated in Fig. 2 by the symbols a and b. The M_S components parallel to the direction of observation in all the Faraday domains have the same value. Therefore

these domains have the same intensity when seen through crossed Nicol prisms.

In the dark domains, the M_S vectors lie in the plane of the plate ("Cotton" domains). The large gray regions correspond to sections of the crystal with multilayer domain structure. The closed domains revealed on the surface of the plate by the powder method are not seen on this photograph, since their volume is small in comparison with the volume of the principal domains. In addition, the magnetization vectors of the closed domains lie in the plane of the plate and therefore contribute to the light-transmission intensity only as a result of the Cotton-Mouton effect, which is weaker in YIG than the Faraday effect by approximately one order of magnitude. The closed domains are therefore not indicated in Fig. 2.

The character of the variation of the domain structure when the plate is magnetized in the $[110]$ direction, which is perpendicular to its plane, is illustrated in Figs. 2a–2d. In order not to complicate the figures, the geometry of the domain structure is shown on the sketches only for the upper surface of the plate. Naturally, the process is analogous in the lower half of the plate and the photographs reflect the summary effect.

The magnetization of the crystal in the region of the domain-wall displacement processes is due principally to restructuring of the Faraday domains (the Cotton domains vanish in very weak magnetic fields). The regions corresponding to the "convenient" domains (domains a in Figs. 2a and 2b) increase at the expense of the domains b. At sufficiently small dimensions, the domains b begin

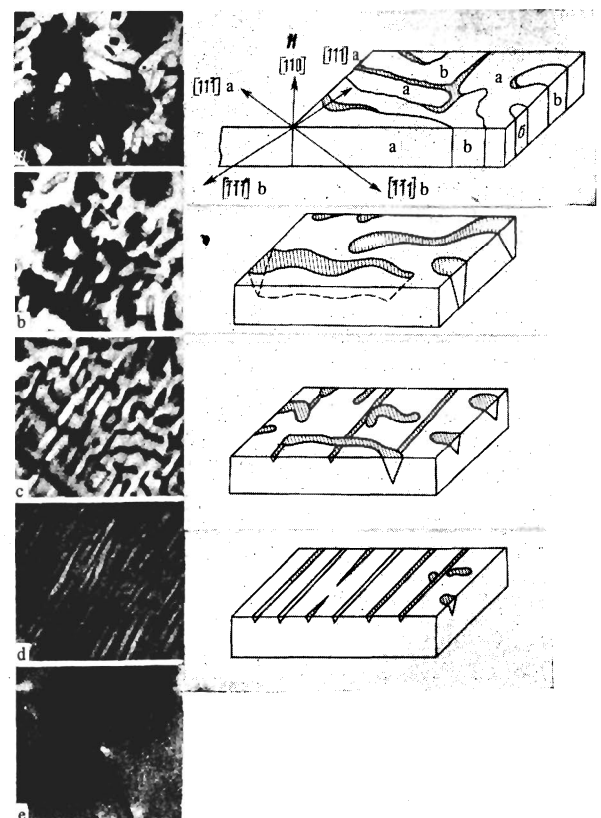


FIG. 2. Change of the domain structure of single-crystal YIG plate following application of an external magnetic field in a direction perpendicular to the plane of the plate (a–d); e—sample magnetized in the plane of the plate. The Nicol prisms are crossed.

to darken (from the boundaries to the center) and break up into smaller "black" domains, which in turn decrease and vanish completely with increasing magnetic field (see Fig. 2d). The darkening of the domains is connected with the following circumstance. Sections of the crystal in which Faraday domains with opposite components M_S^{\parallel} overlap on the light-propagation path, have a weaker intensity because the Faraday effect is odd. Inasmuch as in the neighboring domains the components M_S^{\parallel} are directed oppositely, it follows that in the case of domain boundaries that are inclined relative to the direction of light propagation the dark boundaries on the photographs between the light regions of the domains turn out to be "smeared out." Therefore the gradual darkening of the domains from the boundaries toward the center offer evidence that with increasing dimensions of these domains their shape changes from cylindrical to conical.

With further increase of the magnetic field, simultaneously with the decrease of the dimensions of the conical domains, wedge-like domains appear in the growing domains a on the surface of the plate if the volume of domains a is large enough. In these domains the magnetization vectors are opposite to the direction of M_S of the domains a, as can be easily established by an analysis of the Faraday and Cotton-Mouton effects. These domains appear on the photographs in the form of dark strips in the $[110]$ direction¹⁾. These domains are similar to the near-surface dagger-like domains predicted by E. Lifshitz^[13] for iron crystals in the demagnetized state.

In magnetic fields starting with approximately $H = 1000$ Oe (Fig. 2d), the domain structure consists of a single domain a, which is cut up at the surfaces of the plate by wedge-like domains. With further increase of H , these domains become thinner and shorter, assuming a boat-like shape, and when the field $H \approx 1300$ Oe is reached the crystal becomes single-domain. The magnetization then continues only as a result of rotation of the vectors M_S . When the sample is demagnetized, the first to appear are the wedgelike domains. As will be shown below, they appear primarily at dislocations.

B. Study of the distinguishing features of the behavior of the domain structure and of the rotation of the vectors M_S in the field of microstresses due to an edge dislocation. If the plate with domain structure indicated in Fig. 2a is magnetized in the plane (110) , which is perpendicular to the direction of light propagation, then the magnetic birefringence leads to a uniform transmission of light through the entire crystal. Birefringence rosettes due to the field of stresses around the single edge dislocations parallel to the $[110]$ direction appear against the background of this bleaching of the crystal. Figure 2e illustrates such a state. At the center of the photograph we see one of the rosettes corresponding to a dislocation with a slip plane (110) , which is also the symmetry plane of the rosette. The black and white tone of the rosette is due to the superposition of magnetic birefringence Δn_{m0} on the birefringence Δn_{f0} due to the stress field^[9]. This circumstance enables us to determine the signs of the stresses around the dislocation.

As established earlier in^[9], the magnetization of the YIG, like compressive stresses, transforms it into a uniaxial negative crystal with optical axis coinciding with the direction of the field (or of the compressive stresses). Therefore in the white lobes of the rosette, where the signs of Δn_{m0} and Δn_{f0} coincide, the direction of the

compression stresses coincides with the direction of the magnetizing field (parallel to the horizontal frame of Fig. 2). In the black lobes, on the other hand, Δn_{m0} and Δn_{f0} have opposite signs. Consequently tensile stresses act along H in these sections of the crystal.

Using this fact and the information on the character of the stresses around the edge dislocation^[14], we easily find that the extraplane approaches the dislocation nucleus from the lower left corner of the figure. Maximum compression stresses act in this region and we have maximum tension (acting in the plane of the plate) in the opposite region (relative to the slip plane).

Figure 3 shows the magnetization curves measured in these microscopic regions of compressive (dashed line) and tensile (solid line) stresses. The photometrized sections were in direct contact with the nucleus of the dislocation on both sides of the slip plane, and their diameter was 5μ . In the region where the displacement processes took place, the magnetization curve had a complicated form, due to the fact that the dimensions of the photometrized sections are of the same order as the domain dimensions or even smaller. The magnetization process in this section of the curves is illustrated by the photographs of Fig. 4. Since these photographs were obtained with a smaller magnification, the image of the diaphragm 13 (Fig. 1) on the photograph, which indicates the photometrized area in the region of the tensile stresses, corresponds to a section of 20μ diameter.

FIG. 3. Magnetization curves of YIG crystal microregions adjacent to an edge dislocation parallel to the direction of the magnetic field and subjected to compression (1) and tension (2) stresses. In both cases, the stresses act in planes perpendicular to the direction of the action of the field H (H_n is the field of nucleation (vanishing) of the domains).

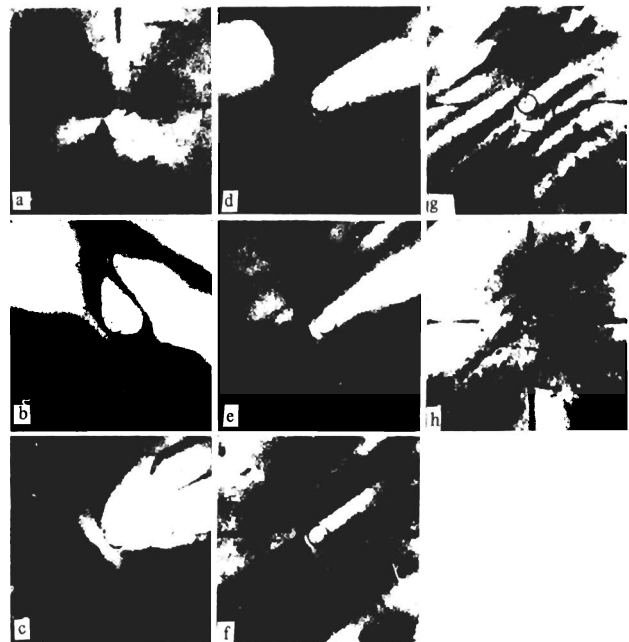
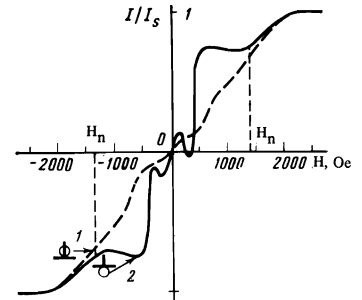


FIG. 4. Character of variation of the domain structure near an edge dislocation in a $Y_3Fe_2O_{12}$ plate (Fig. 2) parallel to the effective magnetic field.

The initial domain structure near the dislocation in the demagnetized crystal is shown in Fig. 4b. On the side of the extraplane there is a Cotton domain adjacent to the dislocation nucleus, and a Faraday domain on the opposite side (relative to the slip plane). Photometry of the light intensity passing through the Faraday domain and a comparison of the result with the transmission through the plate when the latter is magnetized to saturation has made it possible to determine the component M_S^{\parallel} of the vector M_S . The measurements have shown that the M_S in this domain are turned through an angle $55^\circ \pm 0.2^\circ$ relative to the (110) plane, i.e., they coincide with one of the $\langle 111 \rangle$ -type directions.

The domain structure becomes realigned during the course of crystal magnetization, but there is always a Faraday domain in the region of the tensile stresses. The wedge-like domain approaches the dislocation nucleus from the side of the compressive stresses, and on passing through the slip plane the direction of the Burgers vector of the dislocation is shifted by an amount equal to the width of the domain. Since the wedge-like domains near the dislocations are strictly one on top of the other on opposite faces of the plate, and are randomly distributed on the remaining sections of the faces, the image is more contrasty near the dislocation than in the remaining volume of the plate (see Fig. 2d).

When the magnetic field is increased during the stage of the monodomainization, the last to disappear are the domain walls near the dislocation (Fig. 4f). Starting with a field $H \approx 1300$ Oe, only rotations of the vectors M_S take place. The curves of Fig. 3 indicate that the rotation of M_S in a direction perpendicular to the tensile stresses is much faster than in a direction perpendicular to the compressive stresses. When the plate is demagnetized, the nucleation of the (wedge-like) domains begins primarily on the dislocations in a field $H \approx 1300$ Oe.

Thus, the experiment shows directly that the magnetization process near an edge dislocation proceeds in different fashions in different microscopic regions of a ferrimagnet. Such a behavior of the material can be understood by taking into account the magnetic anisotropy induced by the complex stress field; this anisotropy influences the orientation of the vectors M_S . At each point of the volume of the crystal, the minimum of the energy should correspond to the closest orientation of the principal axes of the ellipsoids of the magnetostriction stresses and of the microstresses due to the dislocation. In the case of YIG, which has negative magnetostriction (λ_{100} and $\lambda_{111} < 0$) and four easy-magnetization axes of the type $\langle 111 \rangle$, compressive stresses in any small volume of the sample should separate one of the easy axes making the smallest angle with the direction of action of the stresses (see, for example, experiments on the compression of prisms^[9]). Tensile stresses should separate one of the $\langle 111 \rangle$ directions closest to the plane perpendicular to the direction of the tensile force.

Since the compressive and tensile stresses act in the above-described local sections of the crystal in the plane of the plate, the M_S are directed along the $\langle 111 \rangle$ direction lying in the plane of the plate in the compressed region, and at an angle to it in the stretched region. Consequently a Cotton domain is adjacent to the dislocation nucleus on the side of the extraplane, and is opposed by a Faraday domain.

It should be emphasized that the described singulari-

ties of the behavior of the domains near the dislocation nucleus are not a general rule, and are determined by many factors, primarily by the initial domain structure of the plate^[2]. Nonetheless, the induced local magnetic anisotropy around the dislocation influences the magnetization process during all its stages.

The experimentally observed fact that the laws governing the rotation of the vector M_S vary in different microscopic regions around the dislocation indicates that the distribution of the spontaneous-magnetization vectors is inhomogeneous in this crystal volume even in strong magnetic fields. This creates favorable conditions for the nucleation of the domains near the dislocation during the course of demagnetization of the crystal (see Fig. 4h) from the saturated state. Obviously, the strongly inhomogeneous field of the internal stresses favors the formation of the domains in the case when the increase of the free energy as a result of the surface energy of the produced interdomain walls is offset by the vanishing of the large volume energy of the magnetoelastic anisotropy, which exists in the region of the dislocation when the magnetization is homogeneous. It is therefore natural that dislocation stimulate nucleation of domains when the magnetization of the crystal is reversed in a ferromagnet in which the magnetoelastic energy connected with the dislocation is of the order of the crystallographic-anisotropy energy. The inhomogeneous distribution of the spontaneous-magnetization vectors in the field of the dislocation microstresses is sometimes observed even in a crystal that is broken up into domains. Figure 5a shows the domain structure of a YIG plate displayed in polarized light. In some sections of the crystal one can see bright rosettes of variable intensity. Figure 5b shows a photograph of the same section of the crystal with the Nicol prisms somewhat uncrossed. The extinction of the lobe intensity is evidence that the light in the rosettes is linearly polarized. It is similarly possible to darken the remaining white lobes of the rosettes by rotating the Nicol prism in the opposite direction. If this plate is magnetized in its plane, then the white rosettes are replaced by black-white birefringence rosettes, which are connected with edge dislocations (see Fig. 9a below). The stress field of these dislocations leads to an inhomogeneous distribution of the vectors M_S in the domains surrounding the dislocations, and causes their configuration to differ from that of the domains in the remaining volume of the crystal.

The influence of structure defects on the nucleation of domains in ferromagnetic crystals must be taken into account when a theory of this phenomenon is developed. The predictions of theoretical investigations^[16] carried out without taking into account the role of the crystal imperfections can hardly be realized in pure form in real

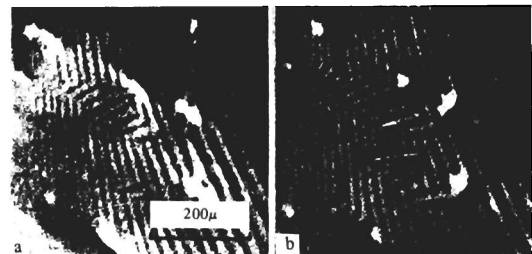


FIG. 5. Appearance of domains with inhomogeneous magnetization in the microstress field around edge dislocations: a—crossed Nicol prisms, b—uncrossed Nicol prisms.

crystals containing dislocations, inclusions, vacancy clusters, and other defects.

Nor is there a detailed theoretical analysis of the rotation process that occurs in the stress field around individual dislocations. Brown^[17] considers this problem only for the concluding stage of magnetization, when the vectors \mathbf{M}_S practically coincide with the direction of the external field. The use of Brown's approximation shows that during this stage of magnetization the elastic field of the dislocations does not influence the character of rotation of \mathbf{M}_S in our case. Such an approximation, however, cannot be used to describe the entire rotation process. Brown's theory explains the experimental results (Fig. 3) only qualitatively.

The force exerted on the vectors \mathbf{M}_S by the stresses can be written in the form

$$f_{\alpha_i} = \partial \Phi_\sigma / \partial \alpha_i,$$

where α_i are the direction cosines of the vector \mathbf{M}_S , Φ_σ is the magnetoelastic energy connected with the stresses, which is described in the isotropic-magnetostriction approximation in the case of a cubic ferromagnet, in a coordinate system xyz that coincides with the fourfold axis, by the formula^[3]

$$\Phi_\sigma = -3/2 \lambda [\sigma_{xx} \alpha_x^2 + \sigma_{yy} \alpha_y^2 + \sigma_{zz} \alpha_z^2 + 2(\sigma_{xy} \alpha_x \alpha_y + \sigma_{yz} \alpha_y \alpha_z + \sigma_{zx} \alpha_z \alpha_x)].$$

In a coordinate system $x'y'z'$ connected with the dislocation (Fig. 4), such that the dislocation line coincides with the z' axis and the Burgers vector with the x' axis, the expression for Φ_σ becomes

$$\Phi_\sigma = -3/2 \lambda [\sigma'_{xx} (\alpha'_x)^2 + \sigma'_{yy} (\alpha'_y)^2 + \sigma'_{zz} (\alpha'_z)^2 + 2\sigma'_{xy} \alpha'_x \alpha'_y],$$

where σ'_{ij} are the components of the stress tensor due to the edge dislocation^[14].

The crystal was magnetized in the direction of the z' axis in sections when the average values of the components σ'_{xy} were negligibly small. Then the deflecting moments of the magnetoelastic forces, which cause the deviation of the vector \mathbf{M}_S from the direction of the external magnetic field, are expressed as follows:

$$f_{\alpha_x} = \partial \Phi_\sigma / \partial \alpha_x = -3\lambda \alpha'_x (\sigma'_{xx} - \sigma'_{zz}), \quad f_{\alpha_y} = \partial \Phi_\sigma / \partial \alpha_y = -3\lambda \alpha'_y (\sigma'_{yy} - \sigma'_{zz}).$$

We see therefore that f_{α_x} and f_{α_y} can accelerate the crystal magnetization in the z' -axis direction or decelerate it, depending on the sign of the stress. This explains the difference in the magnetization curves (Fig. 3) measured in regions of tensile and compressive stresses. The status of the theory, however, does not provide a quantitative estimate of the observed effect.

2. Study of the interaction of the domain walls with unit dislocations

YIG single crystals are multiaxial ferrimagnets. The presence of eight easy-magnetization directions of the $\langle 111 \rangle$ type in YIG makes it possible for different types of domain environments to be produced in the volume of the crystal. In this respect, the YIG is a convenient material for the study of the behavior of the domain boundaries of all possible types. We present below the singularities observed in the interaction of the dislocations with 71° , 109° , and 180° Cotton and Faraday domains.

A. COTTON DOMAINS

a) **180° domains.** Figure 6a shows the photograph of a plate, taken in transmitted linearly-polarized light in

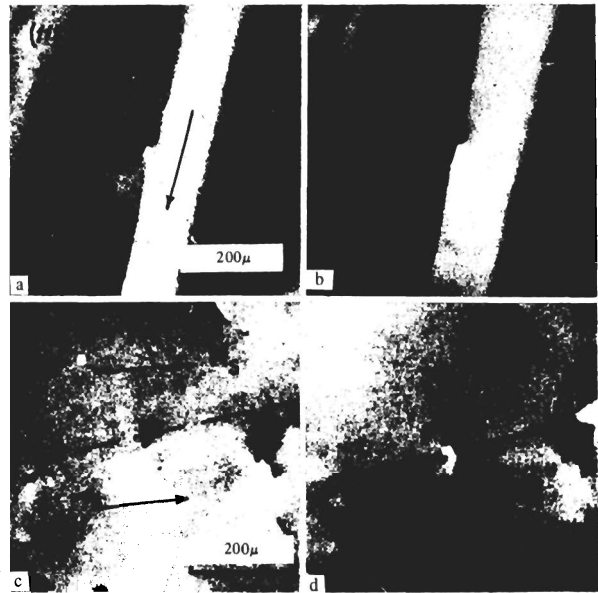


FIG. 6. Interaction of 180° domain walls with atomic dislocations.

the absence of an external magnetic field. At the center of the photograph is displayed a 55° dislocation normal to the (112) plane of the plate. The slip plane of the dislocation is a symmetry plane of the black-white rosette on the photograph and coincides with the $(\bar{1}10)$ plane.

The magnetic structure of this sample consists of domains of 180° environment with magnetization vectors \mathbf{M}_S lying in the plane of the plate and leading to magnetic birefringence. The directions of the vectors \mathbf{M}_S in the domains are determined from an analysis of the signs of the magnetic birefringence in them and the signs of direction of rotation of the plane of polarization in a position when the sample is inclined to the light beam. Under these conditions, there exist parallel components M_S^{\parallel} of the vector \mathbf{M}_S , which are parallel to the direction of light propagation, and which indeed cause the rotation of the plane of polarization. If at the same time the Nicol prisms are uncrossed somewhat, then the domains with opposite magnetizations acquire different tones (dark and light strips in Fig. 6a).

When an external increasing magnetic field is applied to the crystal, the walls between the domains begin to move. Figure 6 shows two positions of the domain wall near a dislocation: when the wall is to the right of the dislocation (Fig. 6a) and to the left (Fig. 6b). We see that on passing through the dislocation the wall does not bend, and its projection remains approximately parallel to the vector \mathbf{M}_S in the neighboring domains. It is noted, however, that the wall moves over the crystal jumpwise and does not remain vertical over its entire path, i.e., it does not remain in the $(\bar{1}10)$ plane, but is appreciably inclined (up to $\sim 10^\circ$) from the normal to the plane of the plate, rotating about the $[11\bar{1}]$ direction parallel to the vector \mathbf{M}_S in the domains, as is evidenced by an analysis of the character of the darkening of the sections of the plate on which the inclined walls are projected.

Thus, it turns out that 180° walls can be easily bent around a direction parallel to the magnetization vector in neighboring domains, and tend to remain parallel to this direction.

We can attempt to explain the absence of a noticeable interaction of the dislocation with the 180° wall by considering the magnetoelastic interaction between the

stress field due to the dislocation and the magnetization in the domain wall. We used for this purpose a method proposed by Seeger et al.^[18], and calculated on the basis of the Pitch-Keller formula the force with which a 55° dislocation acts on a domain wall: here l is the

$$P = \int [dl \times \hat{g}^n] b;$$

dislocation line; \mathbf{b} is the Burgers vector of the dislocation, which in our case is parallel to the [110] direction and equals 17.7 Å; σ^M is the tensor of the additional stresses due to the magnetostriction deformations in the wall. For the most important plane domain walls encountered in the ferromagnetic metals iron, nickel, and cobalt, the tensor \hat{g}^M was calculated by Rieder^[19]. Recognizing that the YIG crystals are similar to nickel in the character of the magnetic anisotropy, we use the results of Rieder's calculations for this crystal.

We choose a coordinate system such that the plane of the boundary and the slip plane of the dislocation coincide with the xy plane, and the dislocation direction coincides with the direction of the x axis. In this case the force in the direction normal to the boundary is

$$P_z = \sigma_{yy}^M l_x b_y + \sigma_{xy}^M l_x b_x;$$

here l_x is the length of the dislocation line along the x axis, equal to the thickness of the plate (0.4 mm), b_y and b_x are the components of the Burgers vector, equal to 14.5 and 10.0 Å, respectively, and

$$\begin{aligned} \sigma_{yy}^M &= \sin \Phi \{ \sin \Phi [\lambda_{100} (-1/4 C_{12}'' - 1/2 \sqrt{2} C_{26}'') + \\ &+ \lambda_{111} (-5/4 C_{12}'' + 3/2 C_{22}'' + 1/2 \sqrt{2} C_{26}'')] + \cos \Phi [\lambda_{100} (1/2 \sqrt{2} C_{12}'' + \\ &+ 2 C_{26}'') + \lambda_{111} (-1/2 \sqrt{2} C_{12}'' + C_{26}'')] \}, \\ \sigma_{xy}^M &= \sin \Phi \{ \sin \Phi [\lambda_{100} (-1/4 C_{16}'' - 1/2 \sqrt{2} C_{66}'') + \\ &+ \lambda_{111} (-5/4 C_{16}'' + 3/2 C_{26}'' + 1/2 \sqrt{2} C_{66}'')] + \cos \Phi [\lambda_{100} (1/2 \sqrt{2} C_{16}'' + \\ &+ 2 C_{66}'') + \lambda_{111} (-1/2 \sqrt{2} C_{16}'' + C_{66}'')] \}; \end{aligned}$$

where

$$\begin{aligned} C_{11}'' &= C_{11}' - C_{13}''/C_{11}', \quad C_{12}'' = C_{12}'(1 - C_{13}''/C_{11}'), \\ C_{16}'' &= C_{16}'(1 + C_{13}''/C_{11}'), \\ C_{22}'' &= C_{22}' - C_{12}''/C_{11}', \quad C_{26}'' = C_{12}'C_{16}'/C_{11}', \quad C_{66}'' = C_{44}' - C_{16}''/C_{11}'; \\ C_{11}' &= 1/2 C_{11} + 1/2 C_{12} + C_{44}, \quad C_{12}' = 1/3 C_{11} + 2/3 C_{12} - 2/3 C_{44}, \\ C_{13}' &= 1/6 C_{11} + 5/6 C_{12} - 1/3 C_{44}, \quad C_{16}' = 1/6 \sqrt{2} C_{11} - 1/6 \sqrt{2} C_{12} - 1/3 \sqrt{2} C_{44}, \\ C_{22}' &= 1/3 C_{11} + 2/3 C_{12} + 1/3 C_{44}, \quad C_{44}' = 1/3 C_{11} - 1/3 C_{12} + 1/3 C_{44}; \end{aligned}$$

The numerical values of C_{ij} , according to Spenser et al.^[20], are

$$C_{11} = 26.9 \cdot 10^{11} \text{ dyn/cm}^2, \quad C_{12} = 10.77 \cdot 10^{11} \text{ dyn/cm}^2, \\ C_{44} = 7.64 \cdot 10^{11} \text{ dyn/cm}^2.$$

and the values of λ according to^[21] are

$$\lambda_{100} = -1.4 \cdot 10^{-6}, \quad \lambda_{111} = -2.4 \cdot 10^{-6}.$$

Substitution of the foregoing constants in the expression for the force yields a quantity

$$P_z \approx -4 \cdot 10^{-3} (870 \sin^2 \Phi + 360 \sin \Phi \cos \Phi) \text{ [dyn]},$$

that depends on the position of the dislocation within the limits of the volume of the wall. The quantity Φ characterizes the angle between the vector \mathbf{M}_S and the y axis inside the wall at the point where the dislocation is located. The maximum value $P_z \sim 4 \times 10^{-2}$ dyn is reached at the instant when the dislocation passes through the center of the wall. A comparison of this force with the force $P_z^H = 2HMS$, with which the magnetic field, acting on the domain boundary, enables it to go through the dislocation, gives an approximate estimate of the elementary coercive force connected with the dislocation: $H_c^0 \approx 0.003$ Oe. This quantity is lower than the minimum jump-like increment of H as specified by us, and naturally could not

be observed in the experiment. In addition, it apparently does not exceed the forces counteracting the motion of the wall and exerted by the other defects (impurity clusters etc.), which determine the jump-like character of the wall displacement.

The energy of the magnetoelastic interaction of the dislocation with a 180° wall, calculated by the Vicena method^[22], do not contradict the foregoing estimates.

Unlike the described case, singularities not predicted by the theories are frequently encountered in interactions between dislocations and 180° walls. Figure 6c shows a photograph taken in linearly polarized light, of a $Y_3Fe_5O_{12}$ plate cut in the (110) plane. Its thickness is 0.1 mm. Against the background of weak illumination through the entire plate, determined by the Cotton-Mouton effect, one sees several black-white birefringence rosettes due to edge dislocations normal to the plane of the plate. The central rosette corresponds to a dislocation with a slip plane (110). The 180° domains present in the crystal, with vectors \mathbf{M}_S lying in the plane of the plate, do not appear on the photograph (the trace of the boundary is indicated by the dashed line). To visualize the domains, the sample must be inclined and the Nicol prisms must be uncrossed, in analogy with the procedure used above.

When the walls pass through a dislocation in an external magnetic field, just as in the former case, no change in its velocity is observed. The domain wall passes over the dislocation freely. However, when the wall approaches the dislocations to an approximate distance equal to 10 μ , two triangular adjacent domains appear on the wall. Figure 6d shows a photograph taken at the instant when the domain wall crosses a dislocation line. One can see at their crossing a small rhombus consisting of two triangles, which have maximum dimensions in this position and indicate the production of two Faraday domains with opposite magnetization on the dislocation. When the wall passes through the dislocation, the rhombus gradually decreases, and at a distance on the order of 10 μ from the dislocation it vanishes.

We shall show that the force of the magnetoelastic interaction a dislocation with a given 180° wall parallel to the (112) plane does not exceed, in accordance with the existing theory, the force calculated for such an interaction in the case of a 180° wall parallel to the (110) plane. By aligning the coordinate plane xy with the plane (112) of the wall, and the edge-dislocation line with the x axis, we obtain an expression for the force P_z in accordance with the Pitch-Keller formula

$$P_z = \sigma_{yy}^M l_x b \cos 55^\circ,$$

where \mathbf{b} is the dislocation Burgers vector parallel to the [001] direction and equal to 12.4 Å; $l_x = 0.1$ mm;

$$\sigma_{yy}^M = [-1/4 \lambda_{100} C_{12}'' + \lambda_{111} (-5/4 C_{12}'' + 3/2 C_{22}'')] \sin^2 \Phi;$$

$$C_{12}'' = 1/3 (C_{11} + 2C_{12} - 2C_{44}) -$$

$$\frac{(C_{11} + 2C_{12} - 2C_{44}) [(C_{11} - C_{12} - 2C_{44})^2 + (C_{11} + 5C_{12} - 2C_{44})(C_{11} - C_{12} + C_{44})]}{9(C_{11} + C_{12} + 2C_{44})(C_{11} - C_{12} + C_{44}) - 3(C_{11} - C_{12} - 2C_{44})^2};$$

$$C_{22}'' = 1/3 (C_{11} + 2C_{12} + 4C_{44}) -$$

$$\frac{2(C_{11} + 2C_{12} - 2C_{44})^2 (C_{11} - C_{12} + C_{44})}{9(C_{11} + C_{12} + 2C_{44})(C_{11} - C_{12} + C_{44}) - 3(C_{11} - C_{12} - 2C_{44})^2}$$

P_z reaches a maximum value $\sim 0.5 \times 10^{-2}$ dyn at $\Phi = 90^\circ$. Such an interaction force, if it really exists, could not be observed in our experiments.

On the other hand, the occurrence of domains of a new phase in the interior of the crystal, where the 180°

wall crosses the dislocation, may be connected to a considerable degree with the magnetic anisotropy induced around the dislocation, to which we already referred, and with the structure of the wall itself. If such a wall is aligned strictly along the direction of light propagation in the microscope and the Nicol prisms are slightly uncrossed, then the wall is revealed in polarized light by white and black strips (Fig. 7). What is most striking is the large thickness of this wall, approximately 10μ . According to Kittel^[23], the thickness of a Bloch wall, expressed in terms of the number of lattice constants, should be

$$N \approx (kT_c / Ka^3)^{1/2},$$

where k is the Boltzmann constant, T_c is the Curie point, K is the anisotropy constant, and a is the lattice constant. As applied to YIG, this yields $N \approx 80$, corresponding approximately to 900 \AA . The experimental value is much larger.

It is quite possible that in YIG single crystals there is realized Vonsovskii's prediction^[23] that a region that is uniformly magnetized along the easy direction, but does not coincide with M_S in the neighboring domains can exist in multiaxial ferromagnetic crystals there can be located between 180° domains. The distinct contours of the wall and the sufficiently uniform intensity over the entire width (Fig. 7) indicate that the magnetization vectors in these sections of the crystal are not distributed in accordance with the law proposed for Bloch walls^[23]. An analysis of the light transmitted along the wall (Fig. 7) shows that the "black" and "white" sections are similar to Faraday domains. When dislocations are crossed, the wall becomes thicker (Fig. 7b).

b) 71° and 109° domains. The character of the interaction of the edge dislocations with the 71° walls that separates the Cotton domains is shown in Figs. 8a–8d. The Cotton domains corresponding on the photograph to two gray regions with different intensities, are observed because the optical indicatrices that characterize the magnetic birefringence in them are rotated in the plane of the plate by an angle equal to the angle between the vectors M_S in the domains. Therefore, for an arbitrary position of the sample relative to the Nicol prisms of the microscope, the Cotton-Mouton effect causes the domains to have different tones. The direction of the vectors M_S in the domains (see Fig. 8c) was determined from an analysis of the magnetic birefringence in them.

The gray regions of the photograph, corresponding to two domains in the crystal, are separated by a darker strip that reflects the projection of the 71° wall on the plane of the plate. The slope of the wall relative to the light beam leads to an overlap, on the path of light propagation, of birefringent media of opposite sign, thus causing an attenuation of the intensity of the field of view. In the region of the right-hand domain (Fig. 8a) one sees at the center of the photograph several black-white birefringence rosettes due to edge dislocations. Figures

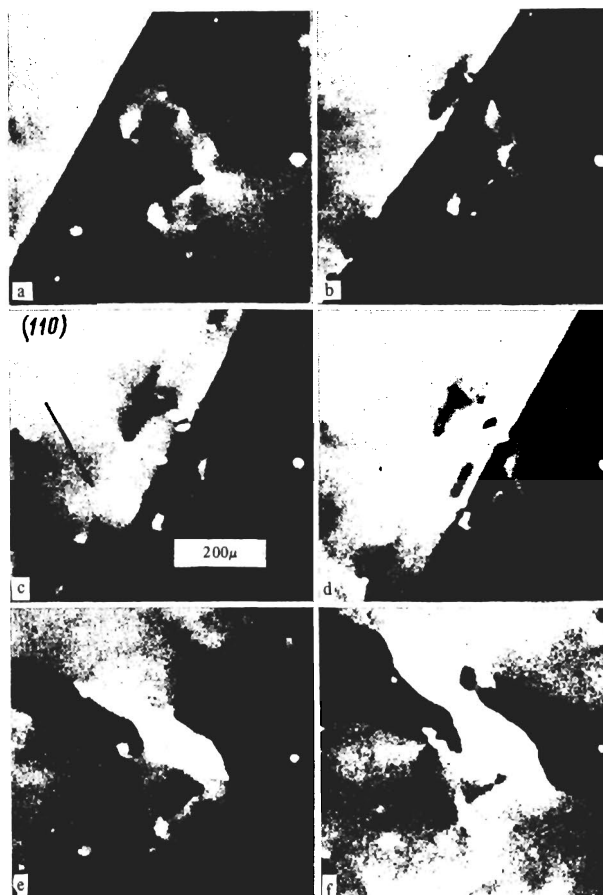


FIG. 8. Interaction of domains of 71° (a–d) and 109° (e, f) environment with edge dislocations.

8a–8d show in succession the positions of the moving 71° wall under the influence of the magnetic field.

We see that the motion of the 71° wall through the volume of a crystal containing a dislocation has produced in this volume two domains, a Faraday domain (white in the photograph) and a Cotton domain (dark). The Faraday domain borders on the right-hand domain and leads to a characteristic kink of the 71° wall (this is clearly seen in Figs. 8c and 8d). When the wall moves away from the dislocation, the Faraday domain, depending on the magnetization condition, can "stretch" behind it over considerable distances. In addition, Figs. 8a–8d show clearly the change in the projection of the wall on the plane of the plate as the wall moves. This means that the 71° wall can deviate from the $(\bar{1}10)$ plane by a 109° rotation about the bisector, produced by the vectors M_S in the neighboring domains, but remains parallel to this direction.

The appearance of domains on the dislocation at the instant when a wall passes through it, and the shapes of the resultant domains, all depend on the direction of motion of the wall and on the magnetization conditions. If the wall shown in Fig. 8d is made to move backwards (to the left), then it will "erase" everything it produced in its forward motion. Such a behavior of the material can be understood qualitatively on the basis of the above-described character of the magnetic anisotropy induced by the field of the microstresses around the dislocation. Cotton and Faraday domains are produced near dislocations in those parts of the crystal where conditions are favorable. A Faraday domain is produced in the region of action of tensile microstresses (just as in Fig. 4),

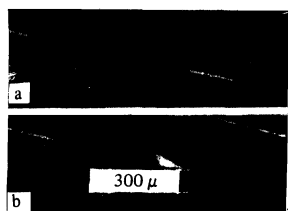


FIG. 7. Fine structure of 180° wall parallel to the (112) plane, displayed in polarized light: a—wall in ideal $Y_2Fe_5O_{12}$ lattice, b—wall intersects an edge dislocation.

and a Cotton domain in the region of tangential stresses. On the other hand, the shapes of these domains, if their volume is large enough, is determined by the condition that the energy of the walls surrounding the domains be a minimum.

It can be assumed that the conditions for the occurrence of these domains near the dislocation are favorable when the volume of the material surrounding it is magnetized in the direction of the vector M_{S1} , not M_{S2} , and therefore the motion of the 71° wall through a dislocation (which is equivalent to a change in the direction of magnetization of the material around it) either creates or annihilates domains of the new phase, depending on the direction of the wall motion. It should also be noted that the initial domain structure of this crystal consists of Faraday domains. The Cotton domains, the boundary between which is shown in Fig. 8, were produced under conditions when the crystal was magnetized with an external magnetic field.

The dependence of the laws governing the production of new-phase domains on their dislocation upon passage of a 71° wall on the magnetization conditions, the type of dislocation, the state of the growth strips in the crystal, and other factors should be investigated further in greater detail. Our experiments, however, already show that domains of a new "magnetic" phase are produced near the dislocation when an edge dislocation interacts with a 71° wall, and kinks appear on the wall itself. Since such kinks lead in essence to an increase in the speed of the wall on one side of the kink (at the instant when the kink is produced) and to a decrease on the other side, this should strongly influence the state of the macroscopic magnetization of the samples. It is precisely such effects (as well as the appearance of Faraday, Cotton, and rhombic domains) which should cause the Barkhausen discontinuities^[3].

As to the magnetoelastic interaction of a dislocation with a 71° wall, estimates show that the strength of such an interaction is of the order of the strength of interaction of a dislocation with a 180° wall.

All the foregoing features of the interaction of a dislocation with a 71° wall appear also in the case of interaction of a dislocation with a 109° wall parallel to (001). The photograph of Fig. 8e is intersected by a strip corresponding to a domain whose magnetization vector M_{S1} makes an angle of 109° with M_{S2} of the neighboring domains. A Faraday domain was produced at the center of this domain by the dislocations (which are displayed in Fig. 8a). At the same time, there are no Faraday domains around the dislocations in domains with vector M_{S2} . The production of such a domain on an individual dislocation when approached by a 109° wall, can be seen near the left-hand rosette of Fig. 8f.

B. FARADAY DOMAINS

According to the general concepts, in ferromagnetic crystals cut in the form of plates parallel to the easy-magnetization direction, domain structure most favored energywise consists of regions magnetized in the plane of the plate. Such a structure contains a minimum number of closing surface domains. However, as shown by investigations, the initial domain structure of real YIG crystals cut in the form of such plates frequently consists of volume Faraday and surface domains. According to our investigations^[15], this is connected with the unique distribution of the point defects which occurs during the

course of crystal growth. Figure 9b shows a polarized-light photograph of a YIG plate cut along the (110) plane and containing Faraday domains. When the Nicol prisms are crossed, these domains are identically colored, but their intensities vary in the transverse direction. The latter circumstance is due to the presence of closed domains of prismatic form on the surfaces of the plate; these domains cause the variable intensity of the Faraday domains. The presence of closed domains is observed by the powder method. Figure 10a shows a photograph of a section of the plate, obtained in polarized light with the Nicol prisms uncrossed. A powder suspension was first deposited over the surface of the sample. The photograph shows clearly that the powder figures, which indicate the emergence of the walls of the closing domains on the surface of the plate, pass through the centers of the Faraday figures. The geometry of the domain structure of this crystal is shown in Fig. 11, where the contours of the Faraday figures are indicated on the surface of the plate above the symbol F, and the contours of the powder figures above the symbol P.

To determine the direction of the vectors M_S in the closing domains, we used the fact that in the initial state the plate consisted of Cotton and Faraday domains. Figure 10b shows a photograph of such a section of the plate. The bulk of the left half of the photograph is occupied by two Cotton domains separated by a 180° wall. The direction of the vectors M_S in these domains was determined

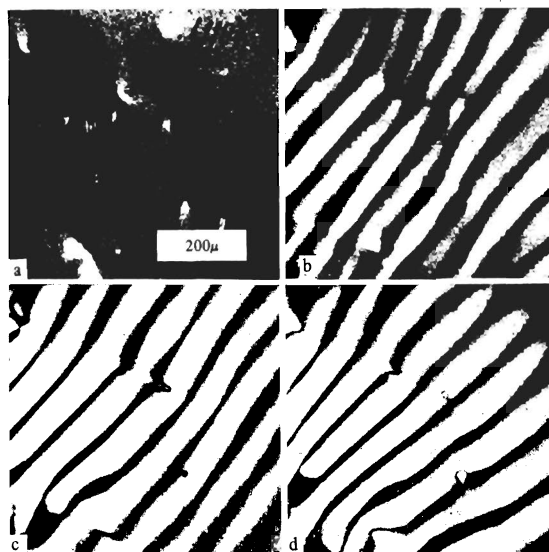


FIG. 9. Interaction of Faraday domains with dislocations perpendicular to the plane of a $Y_3Fe_5O_{12}$ plate: a—crystal magnetized in the plane of the plate, b—d—domain structures after arbitrary magnetization of the crystal (crossed Nicol prisms).

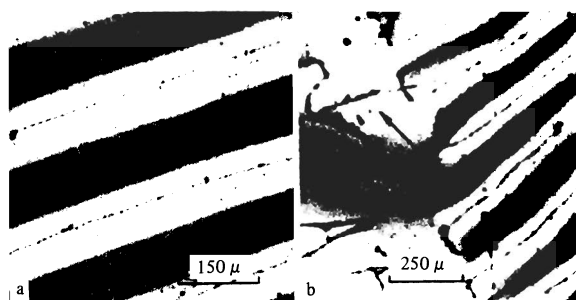


FIG. 10. Domain structure of plate displayed simultaneously by the magneto-optical (light and dark stripes) and powder (thin black lines) methods.

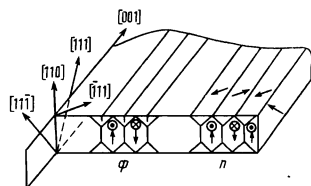


FIG. 11. Schematic diagram of the domain structure in a $Y_3Fe_5O_{12}$, reconstructed on the basis of magneto-optical and powder investigations (Fig. 10).

by the method described above. Adjacent to these domains on the right are Faraday domains, which are differently colored, since the Nicol prisms of the microscope were uncrossed. The powder figures indicate the surface contours of the closing and Cotton domains. It is characteristic that the line of the powder precipitates along the 180° wall between the Cotton domains is not broken on going into the region of the Faraday domains, whereas the closed domains adjacent to these lines are not separated from the Cotton domains by powder figures. This means that the vectors M_S in the closed domains are parallel to the vectors M_S in the Cotton domains. Consequently, on going from one closed domain to another, the vector M_S changes its direction by 180° , as shown in Fig. 11.

If the plate whose domain structure is shown in Fig. 9b is magnetized in the plane of the plate, then the resultant birefringence rosettes (Fig. 9a) reveal that the plate contains several dislocations of different types, normal to the plane of the plate. These dislocations serve as pinning points for the walls separating the Faraday domains.

Unlike all the types of domain walls considered above, the walls shown in Fig. 9b are strongly pinned by the dislocations. It is seen on this photograph that a domain wall was pinned on each of the dislocations displayed in Fig. 9a. The walls are easily bent in the plane of the plate in any direction. Figures 9c and 9d show photographs of the domain structure of this section of the plate after the magnetization of the crystal is reversed. It is seen that the dislocation always tends to capture the boundary. On the other hand, if the coupling between the boundary and the dislocation is broken, then a domain of cylindrical form remains on the dislocation and is magnetized in a direction opposite to the magnetization of the surrounding domain.

We call attention to one other singularity in the behavior of the domain walls shown in Fig. 9. It is seen on the photographs that the interdomain walls tend to lie in the (110) plane, which coincides with the normal to the plane of the plate. When the trace of the wall deviates from the $[100]$ direction, the wall is inclined to the normal (this is manifest in the photograph by broadening of the black boundaries separating the regions corresponding to the Faraday domains). The probable reason is that walls separating domains having opposite magnetizations along the direction $[111]$ or $[\bar{1}\bar{1}\bar{1}]$ (see Fig. 11) always tend to become parallel to the vectors of the neighboring domains. At the same time, the wall remains perpendicular to the plane of the plate (i.e., parallel to the dislocation line) in the field of the stresses around the unit dislocations, regardless of the change of its direction.

The domain walls displayed in Figs. 6a, 6b and 9 are similar in that they lie in the (110) plane and separate 180° domains. Therefore the force of the magnetoelastic

interaction of such a wall with a dislocation, calculated by the method of Seeger et al.^[18] or Vicenna^[22], turn out to be of the same order. The main cause of the difference in the character of their interaction with the dislocations lies apparently in the different orientation of the dislocation axis relative to the magnetization vectors in the neighboring domains, and in the experimentally observed singularities of the behavior of the walls themselves.

In all the domain structures considered above, the domain walls tend to arrange themselves either parallel to the direction of magnetization M_S in the neighboring domains (Fig. 6 and 9), or in such a way that the projections of the vectors M_S on both sides of the walls are the same (Fig. 8). The wall can bend only if these conditions are not violated.

In the experiment we observe the walls in the direction of the dislocation axis. In the case of Cotton domains, their magnetization vectors M_S are perpendicular to the dislocation axis and lie in the plane of the plate. Any bending of the walls in this plane would lead to violation of the noted condition. Judging from the experimental results, in order for this condition to be violated it is necessary to have an energy higher than the energy of the magnetoelastic interaction of the dislocation with the wall. On the other hand, in the case of Faraday domains, the direction of the vectors M_S in the domains is close to the direction of the dislocation line. Such a wall can be bent in the plane of the plate (i.e., around the dislocation) and still kept parallel to the vectors M_S in the domains. Obviously, such a bending of the walls in the microstress field around a dislocation is energetically favored, in spite even of the fact that near the dislocation the domain boundaries are not parallel to the vectors M_S in the neighboring domains. It can be assumed that many factors in the behavior of the walls between Faraday domains are determined by the presence of closed domains in the crystal. Connected with these domains is the energy of the magnetostriction stresses, resulting from the incompatibility of the deformations in the principal and closing domains. Therefore, their location in the crystal can depend strongly on the state of the inhomogeneous internal stresses. On the basis of the existing theories it is impossible to describe the observed singularities of the interaction of single dislocations with the domain structure of ferrimagnetic $Y_3Fe_5O_{12}$ single crystals.

CONCLUSION

Thus, an investigation of the interaction of individual dislocations with the magnetization in domains and domain walls of a known type shows that the theories developed to date do not take into account all the features of the crystal magnetization in the complicated field of dislocation stresses. Even for domain walls of the same type (180° , 71° , or 109°), the character of their interaction with the same dislocation with the same dislocations depends essentially on the mutual placement of the dislocation axis and the directions of the spontaneous-magnetization vectors in the domains. The jumplike character of the magnetization during the initial stages may be due not only to the jumplike character of the motion of the domain walls, which are stopped by the dislocations, but also to nucleation of new domains when a domain wall passes through a dislocation. The regularities of the magnetization during the stage of rotation of the spontaneous-magnetization vector are strongly altered by the stress or dislocation field.

The authors are deeply grateful to S. Sh. Gendelev for supplying the $Y_3Fe_5O_{12}$ single crystals.

¹⁾Their dark tone is due to the considerations advanced above, and the wedge-like form follows from an analysis of the intensity of the tone in direction transverse to the domain: the dark strips become narrower when the nickel prisms are uncrossed.

²⁾The initial domain structure of YIG single crystals depends strongly, in turn, on the density of the dislocations and of other crystal defects [¹⁵].

¹L. D. Landau and E. M. Lifshitz, *Sov. Phys.* **8**, 153, 1935.

²Moderne Probleme der Metallphysik, Ed. A. Seeger, Springer-Verlag, Berlin-Heidelberg-New York, 1966.

³S. V. Vonsovskii and Ya. S. Shur, *Ferromagnetizm (Ferromagnetism)*, GITTL, 1948.

⁴V. I. Nikitenko, L. M. Dedukh, S. Sh. Gendelev, and N. G. Shcherbak, *ZhETF Pis. Red.* **8**, 470 (1968) [*JETP Lett.* **8**, 288 (1968)].

⁵L. M. Dedukh and V. I. Nikitenko, *Izv. AN SSSR ser. fiz.* **34**, 1235 (1970).

⁶V. I. Nikitenko and L. M. Dedukh, *Phys. Stat. Sol. (a)*, **3**, 383, 1970.

⁷V. L. Indenbom and G. E. Tomilovskii, *Dokl. Akad. Nauk SSSR* **115**, 723 (1957); **123**, 673 (1958) [*Sov. Phys.-Dokl.* **3**, 1097 (1959)].

⁸V. L. Indenbom, V. I. Nikitenko, and L. S. Milevskii, *Dokl. Akad. Nauk SSSR* **141**, 1360 (1961) [*Sov. Phys.-Dokl.* **6**, 1034 (1962)]; *Fiz. Tverd. Tela* **4**, 231 (1962) [*Sov. Phys.-Solid State* **4**, 162 (1962)].

⁹S. Sh. Gendelev, L. M. Dedukh, V. I. Nikitenko, and N. G. Shcherbak, *Izv. AN SSSR ser. fiz.* **34**, 1229 (1970).

L. M. Dedukh and V. I. Nikitenko, *Fiz. Tverd. Tela* **12**, 1768 (1970) [*Sov. Phys.-Solid State* **12**, 1400 (1970)].

¹⁰F. Dillon, *J. Appl. Phys.* **29**, 1286, 1958.

¹¹W. C. Elmore, *Phys. Rev.* **54**, 1092, 1938; **62**, 486, 1942.

¹²V. V. Karamzin and V. K. Milevskii, *Opt. Spektr.* **27**, 78 (1969).

¹³E. M. Lifshitz, *Zh. Eksp. Teor. Fiz.* **15**, 97 (1945).

¹⁴J. Friedel, *Dislocations*, Addison-Wesley, 1964.

¹⁵S. Sh. Gendelev, L. M. Dedukh, V. I. Nikitenko, V. I. Polovinkina and E. V. Suvorov, *Izv. AN SSSR ser. fiz.* **35**, 1210 (1971).

¹⁶I. A. Privorotskiĭ, *Usp. Fiz. Nauk* **108**, 43 (1972) [*Sov. Phys.-Uspekhi* **15**, 555 (1973)].

¹⁷W. F. Brown, *Phys. Rev.* **58**, 736, 1940; **60**, 139, 1941; **82**, 94, 1951.

¹⁸A. Seeger, H. Kronmüller, H. Rieger and H. Träuble, *J. Appl. Phys.* **35**, 740, 1964.

¹⁹G. Rieder, *Abhandl. Braunschweig Wiss. Ges.*, **11**, 20, 1959.

²⁰E. G. Spenser, R. T. Denton, T. B. Bateman, W. B. Snow and L. C. Van Uiter, *J. Appl. Phys.* **34**, 3059, 1963.

²¹E. de Lacheisserie and J. L. Dormann, *Phys. Stat. Sol.* **35**, 925, 1969.

²²F. Vicena, *Czech. J. Phys.* **4**, 419, 1954; **5**, 11, 1955; **5**, 480, 1955.

²³C. Kittel, *Rev. Mod. Phys.* **21**, 541, 1949.

Translated by J. G. Adashko

41